

Pool Boiling Heat Transfer from Aluminum Alloy Circular Surface Using Al_2O_3 and CuO Water Based Nano-fluids

Adel A. Fahmy^{1*}, Ali A. Abdel Aziz²

¹ Nuclear Reactors Department, Egyptian Atomic Energy Authority, P.O.B. 13759, 11787 Cairo, Egypt

² Department of Mechanical Power, Faculty of Engineering, Benha University, P.O.B. 11629, 11637 Cairo, Egypt

* Corresponding author, e-mail: adel.alyan@eaea.org.eg

Received: 07 March 2019, Accepted: 18 July 2019, Published online: 01 October 2019

Abstract

The present work aims to study the effect of nano-particles volume fraction of nano-fluid on the heat transfer during pool boiling with different values of heat flux. The concentration ratios by volume in demineralized water are taken as 0.02 %, 0.20 %, 0.40 %, 0.60, and 0.80 % for Al_2O_3 nano-particles and 0.02 %, 0.06 %, and 0.20 % for CuO nano-particles. Heat transfer coefficients for pool boiling were established experimentally for different values of volume fraction and heat flux. The heating element is made from an aluminum alloy (AL 6061) with a circular smooth surface of 100 mm diameter and 10 mm thickness. The nano-particles porous layer that builds up during boiling is observed by a scanning electron microscope of the heated surface before and after the boiling. The results demonstrate that the heat transfer rate depends on the concentration ratios and heat flux. Using nano-particles decreases the pool boiling heat transfer in comparison with demineralized water. Due to the deposition of nano-particles on the heated surface, lower heat transfer is obtained for a lower bubble departure compared with demineralized water for the small wall superheat.

Keywords

nano-fluids, boiling heat transfer, alumina nano-particles

1 Introduction

Ahmad et al. [1] investigated the surface characteristic effect and electrostatic field on the rate of heat transfer and their critical heat flux for pool boiling of R-123 at 1 bar with saturation condition. A sandblasted cylindrical copper block was used with embedded electric heating elements and standardized surface roughness parameter (3.5 μm). The results showed that the rough surface has a significant effect on increasing in the heat transfer rates when compared with a smooth surface. A further increase in the heat transfer rates is produced by electric field effects for lower values of heat flux. Experimental investigation of pool boiling heat transfer of water- Al_2O_3 and water-Cu nano-fluids has been carried out by Cieslinski and Kaczmarczyk [2]. Nano-particles were established at the concentration of 0.01 %, 0.1 %, and 1 % by weight. The tested tubes were smooth copper and stainless steel and in horizontal position and have 10 mm outer diameter and 0.6 mm wall thickness which formed test heater. The experiments have been performed to show the influence of nano-fluids concentration as well as tube surface material on heat transfer characteristics at atmospheric

pressure. No influence on the heat transfer coefficient is noticed while boiling of water- Al_2O_3 or water-Cu nano-fluids on smooth copper tube i.e, the material of the heater did not affect the boiling heat transfer coefficient in 0.1 wt.% water-Cu nano-fluid. Higher heat transfer coefficient was reported distinctly for stainless steel tube than for copper tube for the same heat flux density. Pal and Bhaumik [3] reported that approximately 22 % increase in heat transfer coefficient is observed for 0.72 wt.% nano-particle. Ribatski and Thome [4] presented an experimental analysis of heat transfer through pool boiling of R134a on different tubes for a wide range of high heat flux from 20 to 70 kW/m^2 and three different saturation temperatures of 5, 10, and 20 °C. Their results showed that the effect of saturation temperature has no significant effect on the heat transfer coefficient except for Turbo-CSL while for increasing the heat flux, a slight noticeable decrease in heat transfer coefficient or an almost constant value are observed. An overview has been presented by Kavitha et al. [5] for some developments in nano-fluids such as the preparation methods, the evaluation methods for their

stability, the ways to enhance their stability, the stability mechanisms, and their potential applications in heat transfer intensification, mass transfer enhancement, energy fields, mechanical fields and so far. The performance of nano-fluid critically depends upon the size, quantity (volume percentage), shape and distribution of dispersions, and their ability to remain suspended and chemically un-reacted in the fluid. It was found that MgO-EG nano-fluid have the lowest viscosity and the highest thermal conductivity [5]. Cieśliński and Kaczmarczyk [6] conducted pool boiling of water – Al_2O_3 and Cu nano-fluids on rough and porous coated horizontal tubes. The surface of testing tubes was roughed by using emery paper 360 or polished with abrasive compound. Aluminium porous coatings of 0.15 mm thick with porosity of about 40 % were produced by plasma spraying. Different absolute operating pressures have been used, i.e., 200, 100, and 10 kPa. Nano-particles were verified at the concentration of 0.01, 0.1, and 1 % by weight. The dispersion of the nano-particles is stabilized by using Ultrasonic vibrator. The results showed that that independent of operating pressure and roughness of the stainless steel tubes addition of even a small amount of nano-particles augments heat transfer in comparison to boiling of demineralized water. Opposing to rough tubes boiling heat transfer coefficient of testing nano-fluids on porous coated tubes was lower compared to that of demineralized water while boiling on porous coated tubes. For large values of heat flux surface, the enhancement of heat transfer can be achieved. Many studies have been done to improve the heat transfer during the pool boiling through nano-fluid by Ciloglu and Bolukbasi [7]. Salari et al. [8] studied experimentally the thermal performance of alumina nano-fluids during the quenching process of a surface at the boiling condition. They prepared their own nano-fluids by dispersing the 5, 50 and 80 nm alumina nano-particles into the deionized water. The experiments are divided into two domains, namely the short time study and the extended time study. For the short time study (0-60 minutes) heat transfer coefficient enhancement has been reported for all nano-fluids, however for nano-fluid with smaller nano-particle size, heat transfer coefficient is found to be considerably deteriorated for all nano-fluids in the extended time study (60:1000 minutes). Ali et al. [9] investigated the nucleate pool boiling heat transfer enhancement of TiO_2 -water based nano-fluids experimentally. They concentrates on the impact of TiO_2 -water based nano-fluids on the wall superheating, boiling heat transfer coefficient, and heat

flux at atmospheric pressure. Two different concentrations of 12 % and 15 % by weight of TiO_2 in water as a base fluid were tested. Boiling heat transfer coefficient enhancement was found to be 1.38 and 1.24 for 15 % TiO_2 and 12 % TiO_2 nano-fluids respectively in comparison with the demineralized water. Kshirsagar and Shrivastava [10] conducted experimentally the nucleate pool boiling characteristics of high concentrated alumina/water nano-fluids. They studied the critical heat flux (CHF) and boiling heat transfer coefficient of alumina nano-particles. 0.3, 0.6, 0.9, 1.2 and 1.5 wt% concentration was selected. The critical heat flux enhancement rate decreases as concentration increases is observed as a result. After 1.2 wt% concentration of nano-fluids, the surface roughness of heater surface decreases. Moreira et al. [11] analyzed the heat transfer performance of nano-fluids under single phase flow, pool boiling and flow boiling conditions. The results found that the heat transfer coefficient of single-phase flow is enhanced by the addition of nano-particles to base fluids. W.r.t the pool and flow boiling conditions, the heat transfer coefficient either increase or decrease.

Nazari and Saedodin [12] studied experimentally the nano-fluid pool boiling on the aluminium surface at different volume fractions which are 0.002, 0.01, 0.05 and 0.1 vol.%, the results showed that by adding the nano-particles, the critical heat flux increase at a certain concentrations. A critical heat flux has maximum enhancement reached to 19 %. The effect of wettability, roughness and thickness of deposited nano-particles on the critical heat flux have been studied. Saad and Lezsovits [13] carried out a review of recent studies on boiling heat transfer of nano-fluids for pool and convective flow boiling of nano-fluids. The research results, collected since 2012 to present of the recent survey have been reviewed. The enhancement and the deterioration of the boiling heat transfer coefficient and critical heat flux of the pool and convective flow boiling of nano-fluids are briefed.

In this paper, an experimental study was carried out to investigate the pool boiling heat transfer characteristics, i.e. a surface scanning electron microscope, boiling curves, and heat transfer coefficients coefficients for water- Al_2O_3 and water-CuO nano-fluids of different nano-particle concentrations while boiling on a circular plain surface of a nuclear grad cladding material, aluminum alloy (Al 6061) with dimension of 100 mm outside diameter and 10 mm thickness. The concentrations of nano-particles were investigated at volume fraction, 0.02 %, 0.20 %, 0.40 %, 0.60, and 0.80 % for Al_2O_3 nano-particles and

0.02 %, 0.06 %, and 0.20 % for CuO nano-particles. The novelty of the present work lies in using a nuclear grad cladding material as a heating surface with different nano-particle concentrations, in addition of calculation of active nucleation site density for a cladding material, aluminum alloy (Al 6061) in pool boiling.

2 Experimental boiling facilities

To achieve the aforementioned requirements, a test rig has been designed, manufactured and constructed in which nucleate pool boiling of nano-fluid solutions could be achieved on the electrically heated horizontal circular plain surface. The experimental set up, as shown in Fig. 1, consists of an aluminum alloy (Al6061) main heating surface where boiling occurs, a housing vessel to contain the fluid, and a condenser section. An aluminum alloy (Al 6061) circular plain smooth horizontal surface of 100 mm outside diameter and 10 mm thickness was used. The heat source is a cylindrical bar of 85 mm diameter. The heating element input power is controlled by a voltage regulator (2 kW, 0-250 V, 10 A). The heater is mated to a stainless steel disc, 85 mm in diameter and 3.5 mm in thickness. This assembly is embedded in a thermal insulator housing composed of Teflon 130 mm in diameter and 14 mm in thickness. This housing is packed with glass wool insulation to minimize the heat losses to the ambient. The losses can be neglected in radial direction due to the insulating sleeve and most of the heat conducted in vertical direction to the horizontal plate that will be transferred to the nano-fluid. The bottom side of the heating element was insulated with a Teflon cap where the heat loss calculated by conduction from this side to the atmosphere was found about 5 % of the total heat input. The working fluid is contained in a stainless steel vessel housing that has a chamber 160 mm in diameter and 210 mm in the heights. During the experiments the vapor condensed onto

the surface of a copper coil at the top. The cooling water inlet flow rate to the coil was controlled to maintain a constant condensation pressure and the corresponding saturation temperature. This is accomplished by continuously control on the temperature difference between the bulk temperature of the test nano-fluid solution and the inlet cooling water temperature. The temperature of the boiling surface was measured by four thermocouples (type T) embedded at 1.0 mm below the heating surface and distributed radially. The average temperature of the heating surface used to calculate the heat transfer coefficient. At steady state condition the average surface temperature and the heating power to the heating surface are recorded. The pool fluid temperature (saturation temperature) was measured by using a T-type thermocouple embedded from the bottom. The measured value of the saturated temperature corresponding to the measured saturated pressure changes with the concentration of nano-fluid. The instrumentation was interfaced with a computer and data acquisition system with Pico Log software to monitor and display all thermocouples using a waveform chart to illustrate the steady state condition. The pool boiling detailed geometry of the experimental setup is shown in Fig. 2.

2.1 Nano-fluid properties

In the present study, Al_2O_3 and CuO were used as a nano-particle while demineralized water was used as a base fluid. The reasons for choosing these nano-particles are that they are commercially cheap and widely used in this

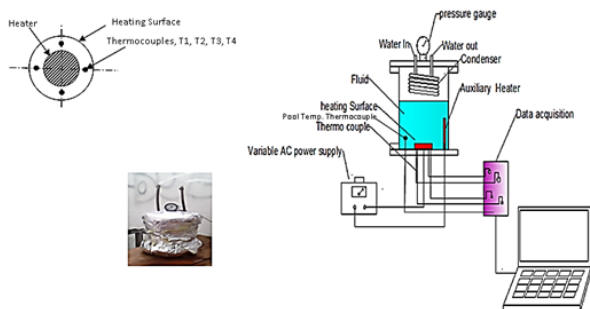


Fig. 1 Pool Boiling Experimental Set up

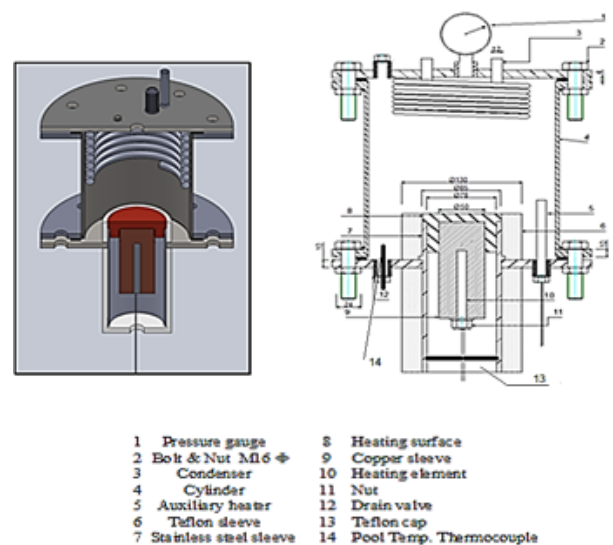


Fig. 2 Details of pool boiling vessel and schematic of heat source assembly

research area owing to requirements, continuous suspension without any outstanding chemical change of the base fluid. Alumina and copper oxide nano-particles have a spherical shape of about 40 nm average diameter, which is given by Inframat® Advanced Materials Corporation, USA (99.99 % purity, product code 26N-0801G, 40 nm average particle size with surface area with more than 200 m²/g). Alumina and copper oxide nano-fluids with different mass concentrations for the experiment were prepared by controlling the amounts of the particles. The nano-fluids are prepared to provide a stable suspension of nano-particles in the base liquid. The nano-particles are measured and added to a container containing 1 liter of demineralized water to achieve the desired concentrations. The solution is stirred with a magnetic stirring device. Fig. 3 shows the photograph of Al₂O₃ and CuO nano-fluid with 0.2 % volume fraction that was prepared in the lab. Fig. 3 shows that Al₂O₃ and CuO nano-particles are well dispersed into base fluid. A mechanical vibrator was used to mix the nano-particles uniformly into the base fluid for about one hour.

The volume fractions of nano-particles are written as:

$$\varphi = \frac{1}{\left[\left(\frac{1-\varphi_m}{\varphi_m} \right) \frac{\rho_p}{\rho_f} + 1 \right]} \quad (1)$$

The density of a nano-fluid can be calculated by using mass balance as:

$$\rho = \rho_f (1-\varphi) + \rho_p \varphi \quad (2)$$

The specific heat of a nano-fluid can be calculated by using energy balance, Xuan and Roetzel [14] as:

$$C_p = \frac{\rho_f C_{pf} (1-\varphi) + \rho_p C_{pp} \varphi}{\rho} \quad (3)$$

The thermal conductivity of the solution can be easily calculated through a Maxwell model [15] without considering the temperature effect by Eq. (4):

$$k = \left[k_p + 2k_f + 2(k_p - k_f)\varphi \right] / \left[k_p + 2k_f - (k_p - k_f)\varphi \right] \quad (4)$$



Fig. 3 Al₂O₃ and CuO – water based nano-fluid of 0.2 % volume fraction

The thermo-physical properties of Al₂O₃ and CuO nano-particles are shown in Table 1.

2.2 Data reduction

The electric power supplied to the plain heater (*P*) is used to compute the heat flux by Eq. (5):

$$q = IV \cos\theta / (\pi D^2 / 4) \quad (5)$$

where *V* and *I* are the voltage and current across the heater, respectively, $\cos\theta$ is the power factor ($\cos\theta = 0.98$), *D* is the circular plain surface outer diameter. The average boiling heat transfer coefficient is calculated from the heat flux calculation in Eq. (5), the average measured surface temperature and the bulk fluid temperature (which is the saturation temperature) is calculated by Eq. (6):

$$h = \frac{q}{(T_w - T_{sat})} \quad (6)$$

2.3 Experimental procedure

The nucleate boiling heat transfer characteristics of nano-fluids with nano-particles suspended in water are tested at a constant heat flux from 37 to 129 kW/m² and saturation pressure of 101.3 kPa. Before each run, nano-fluid at a preset concentration is charged and then pre-heated to the saturated temperature. First measurement is performed at different values of power input. The data are then collected by increasing the heat flux by small increments while the saturation pressure is kept constant at the pre-selected value. If the variation of saturation temperature is smaller than 273 K in 5.0 min, the heat transfer process can be considered to reach a steady state and each data point are taken at steady state. Five temperatures on the boiling surface and saturation temperature in the nano-fluid were recorded. Before changing the concentration, the test surface is cleaned with acetone to remove the sticking nano-particles, ensuring no change of the test surface characteristics. Estimating Uncertainties of the measured and calculated parameters in experimental results has been presented by Kline and McClintock, which is mentioned in Holman [16].

Table 1 Major properties of nano-fluids

	Al ₂ O ₃				CuO			
φ_v (%)	0.02	0.20	0.40	0.60	0.80	0.02	0.06	0.20
ρ/ρ_f	1.00	1.00	1.01	1.02	1.02	1.00	1.00	1.00
k/k_f	1.01	1.11	1.23	1.34	1.46	1.01	1.03	1.11

The heat flux density was calculated from Eq. (5). The experimental uncertainty of heat flux density and average heat transfer coefficient were estimated by Eq. (7):

$$u_q = \sqrt{\left(\frac{\partial q}{\partial I} u_I\right)^2 + \left(\frac{\partial q}{\partial V} u_V\right)^2 + \left(\frac{\partial q}{\partial A} u_A\right)^2} \quad (7)$$

Calculations of the heat transfer coefficient depend on the heating surface and nano-fluid average temperatures as a result the uncertainty of temperature reading is needed to calculate the heat transfer rate. An accurate standard temperature device of ± 0.1 °C accuracy was used to calibrate the thermocouples in the lab. The temperature difference between the heating surface and the saturation temperature of the nano-fluid $\Delta T = T_w - T_{sat}$, its uncertainty $U \Delta T$ is obtained by Eq. (8):

$$u_{\Delta T} = \pm \sqrt{\left(\frac{\partial \Delta T}{\partial T_w} u_{T_w}\right)^2 + \left(\frac{\partial \Delta T}{\partial T_{sat}} u_{T_{sat}}\right)^2} \quad (8)$$

$$= \pm \sqrt{(1 \times 0.1)^2 + (-1 \times 0.1)^2} = \pm 0.14 \text{ } ^\circ\text{C}.$$

The uncertainty in the heat flux transfer rate from the heating surface to the nano-fluid is ± 2.6 %. The uncertainty in heat transfer coefficient is calculated from:

$$\frac{u_h}{h} = \pm \sqrt{\left(\frac{u_q}{q}\right)^2 + \left(\frac{u_{\Delta T}}{T_{sat} - T_w}\right)^2} = \pm 5.2 \text{ } \%. \quad (9)$$

The maximum relative uncertainty of nucleate pool boiling heat transfer coefficient was (5.2 %) at maximum saturation temperature condition.

3 Results and discussion

In order to check the reliability of the apparatus, the present experimental results for the pool boiling heat transfer coefficient of demineralized water without adding nano-particles were compared to the experimental results reported by Gerardi et al. [17] at various values of heat flux as shown in Fig. 4. The present results are well within the Gerardi's results and the trends confirm the validity of the present experimental measurements. Pool boiling curves were generated for demineralized water and nano-fluid with different concentrations of Al_2O_3 and CuO . Generally the heat transfer results show that the pool boiling heat transfer coefficients for all nano-fluids are lower than that of pure water. An analysis of the Aluminum alloy heating surface has been observed by a scanning electron microscope before and after pool boiling. The roughness of the smooth, heating fresh surface with no polishing is closely equal to $0.5 \text{ } \mu\text{m}$ before pool boiling. In addition,

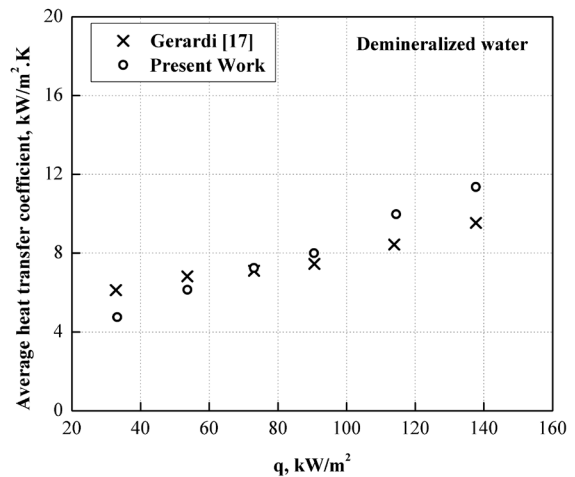


Fig. 4 Comparison of the present results with Gerardi et al. [17]

Fig. 5 shows an optical microscope image of the clean heating surface. It is observed that there are a machining grooves and cavities of varying shapes and sizes distributed along the heating surface. After pool boiling in Al_2O_3 nanofluid, a qualitative observation of the heated surface was noticed where the heating surface was prepared for SEM. A porous layer builds up due to precipitation of some nano-particles where the average and maximum roughness of heating surface are closely to about $12.5 \text{ } \mu\text{m}$ and $28 \text{ } \mu\text{m}$, respectively. Figs. 6 and 7 show an optical microscope image at different locations at the center and at the edges of the heating surface after nano-fluid boiling tests 0.8 % and 0.2 % for Al_2O_3 and CuO nano-fluids, respectively. The porous nano-particle layers deposited during nucleate boiling at the center have a different shapes and sizes in comparison with that at the edges. These irregular porous nano-particle layers affect the nucleate boiling phenomena heat transfer by changing the surface area, wettability, and roughness. The roughness of the surface boiled in nano-fluid is about twenty five times higher than those of the fresh surface before boiling in nano-fluid. When the size of the particles and the size of the surface roughness are comparable, the particles settle in the voids of the surface and block nucleation sites

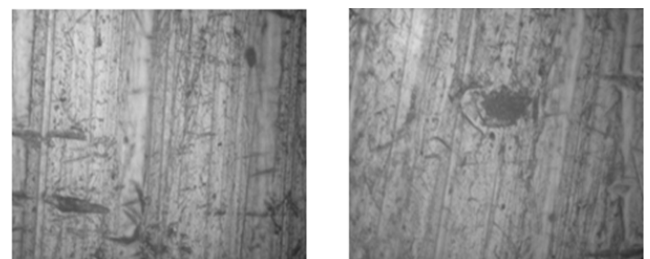


Fig. 5 Optical microscope images before pool boiling

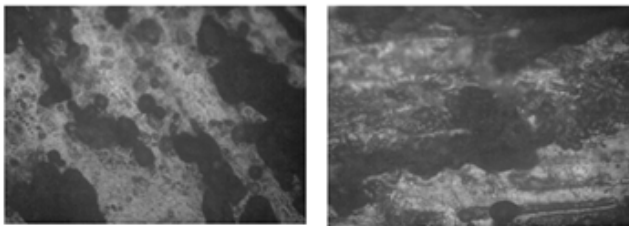
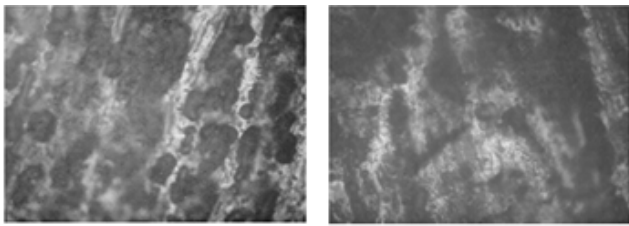


Fig. 6 Optical microscope images after pool boiling in Al₂O₃ nanofluid 0.8 % by Vol.

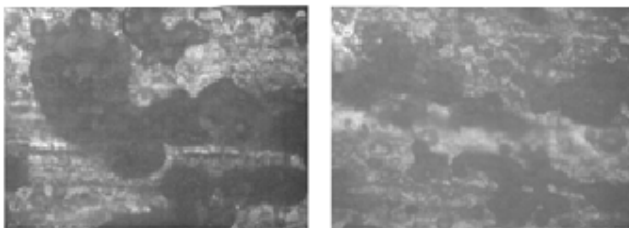
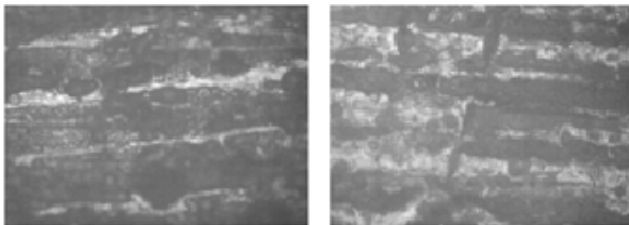


Fig. 7 Optical microscope images after pool boiling in CuO nano-fluid 0.2 % by Vol. (a) at the center 50 X (b) at the edge 50 X

which lead to heat transfer deterioration Cieslinski and Kaczmarczyk [18]. It is found that the effect of increased surface roughness due to nano-particle layering can be twofold, significantly reducing boiling of the base fluid and slightly decreasing performance for the nano-fluid.

3.1 Effect of saturation temperature on heat flux

Commissioning tests of the boiling facility were conducted using demineralized water over several days. In each case, the cylinder vessel was maintained at atmospheric pressure and held at saturation conditions. To provide an example of studying modified boiling heat flux conditions, data measurements were collected for both nano-fluids (Al₂O₃ and CuO). Before applying any voltage to the heater, the fluid level was marked on the vessel

container. Once the experiment started, vapor began to escape slowly. The prepared nano-fluids were vibrated for one hour before adding into the test vessel through the tubing valve in an effort to keep the nano-fluid concentration in stabilization and homogenous. In this experimental investigation, boiling heat flux curves using demineralized water were generated and compared to curves generated from nano-fluids with 0.02 %, 0.06 %, 0.20 %, 0.40 %, 0.60 %, and 0.80 % volume concentrations under the same conditions. The heat flux density and heat transfer coefficient of demineralized water and the nano fluids are compared through the experimental test for different values of concentration level. The heat flux and the temperature of the nucleate boiling are measured for demineralized water and the nano-fluids as shown in Fig. 8.

Addition of alumina nano-particles caused the water boiling curve to shift to the right, i.e. an increase of wall temperature and a decrease of pool nucleate boiling heat transfer. For same heat flux, the wall temperature for all nano-fluids concentrations are higher compared with the demineralized water. This shows that the heat transfer coefficient was decreased by increasing particle concentration.

It could be said that the heat transfer coefficient is lower than the water base fluid and decreases when the concentration increases. These results are consistent with the findings of Das et al. [19] and Bang and Chang [20], where a low nucleate heat transfer coefficient is found with a high heat flux for nano-fluids. Fig. 9 shows pool boiling curves for water-CuO nano-fluid of different concentrations (0.02 %, 0.06 %, and 0.20 % by volume). Generally at constant heat flux and atmospheric pressure, an increase of nano-particle concentration of 0.02 %, 0.06 %, and 0.20 %,

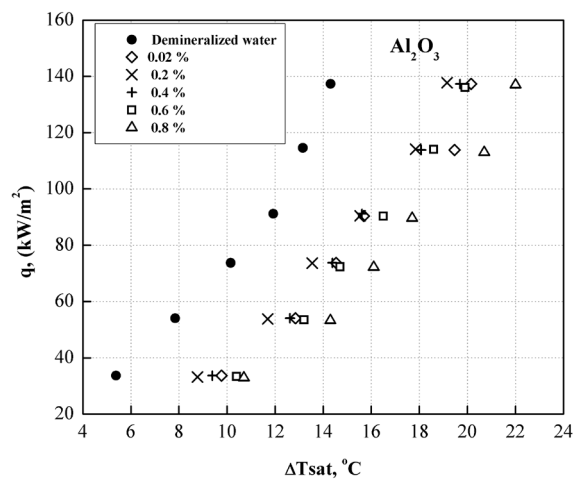


Fig. 8 Pool boiling curve of water- Al₂O₃ nano-fluid for different values of volume concentration

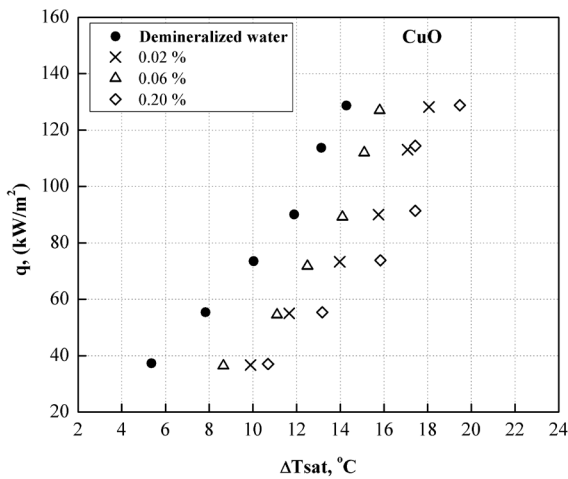


Fig. 9 The pool boiling curve of CuO nano-fluid at different volume fraction

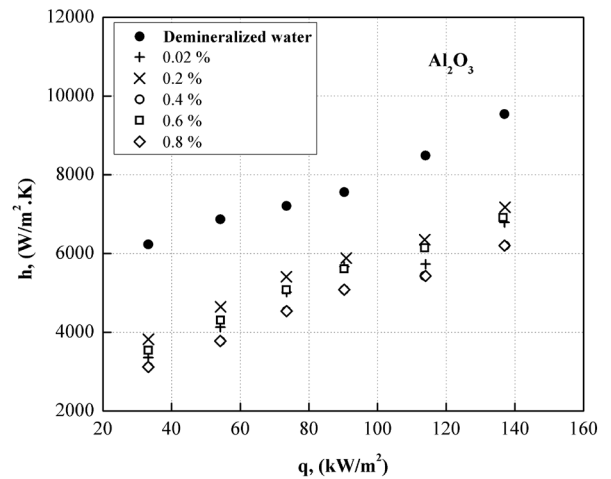


Fig. 10 Boiling heat transfer coefficient of Al₂O₃ nano-fluid for different volume fraction

the average measured surface temperature increases and causes a decrease of pool nucleate boiling heat transfer. The surface of the heating element was clean during demineralized water boiling, but a porous layer built up during nano-fluid boiling. The presence of a porous nano-particle layer due to particle deposition during nucleate boiling causes the increasing in the surface temperature. At atmospheric pressure, a more significant effect of the concentration on the surface temperature is observed for water-CuO nano-fluid than that for water- Al₂O₃ nano-fluid.

3.2 Effect of heat flux on heat transfer coefficient

Fig. 10 illustrates the variation of heat transfer coefficient against the heat flux density for Al₂O₃ nano-fluid with different values of nano-particle concentration. The pool boiling heat transfer coefficient of Al₂O₃ nano-fluid is reduced by a maximum value of 43 % for a given wall heat flux density compared with the demineralized water. The heat transfer coefficient increases as the heat flux density increases and for a given heat flux, the heat transfer coefficients at various nano-particle concentrations are closer together than those on the demineralized water. Nano-particle layers fully cover the heating surface increases thermal resistance which decreases its heat transfer coefficient.

Fig. 11 shows the variation of the heat transfer coefficient with heat flux density for CuO nano-fluid with different values of nano-particle concentration. It can be seen that the heat transfer coefficient increases with increasing heat flux for both demineralized water and nano-fluid. The nucleate pool boiling heat transfer coefficient of demineralized water and CuO nano-fluid were compared for different concentrations as shown in Fig. 11. Different concentrations of CuO

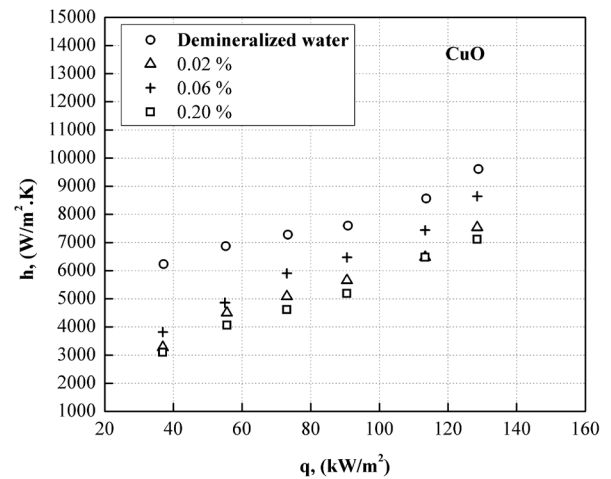


Fig. 11 Boiling heat transfer coefficient of CuO nano-fluid at different volume fraction

nano-fluid display different degrees of deterioration in boiling heat transfer. At the same heat flux, the heat transfer coefficient is lower than that for demineralized water across the range of heat flux. These decreases are due to the surface effects and the surface roughness produced by nano-particle layering. Fig. 12 illustrates the heat transfer coefficient versus heat flux density of water- Al₂O₃ and water-CuO nano-fluids of 0.02 % volume fraction. A higher heat transfer coefficient was obtained for demineralized water.

3.3 Nucleation site

Active nucleation site density for the surface in pool boiling was estimated by Mikic-Rohsenow model [21] that based on the transient heat conduction mechanism such that:

$$q = 1/2(\pi k_f \rho c_p)^{1/2} f^{1/2} D_d^2 N_a (T_s - T_{sat}). \tag{10}$$

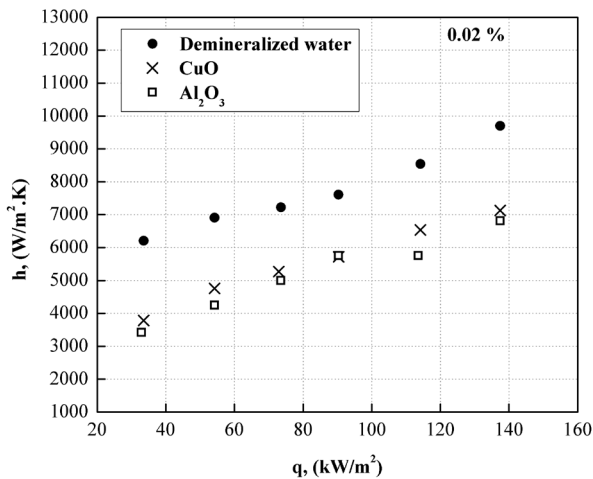


Fig. 12 Boiling heat transfer coefficient versus heat flux density of water- Al_2O_3 and water-CuO nano-fluids of 0.02 % volume fraction

The active nucleation site density depends on the bubble departure diameter and frequency which are modelled as functions of fluid properties.

$$D_d = 1.5 \times 10^{-4} \left[\frac{\sigma}{(\rho - \rho_v)} \right]^{1/2} \left(\frac{\rho c_p T_{sat}}{\rho_v h_{fg}} \right)^{5/4} \quad (11)$$

$$fD_d = 0.6 \left[\sigma (\rho - \rho_v) / \rho_v^2 \right]^{1/4} \quad (12)$$

The active nucleation site density of the heating surface in this present work is calculated from Mikic-Rohsenow model [21] correlation:

$$N_a = \frac{q}{\frac{1}{2} (\pi k_l \rho c_p)^{1/2} f^{1/2} D_d^2 (T_s - T_{sat})} \quad (13)$$

The nucleation site density using Eq. (13) based on the experimental data is plotted against the heat flux as shown in Figs. 13 and 14 for Al_2O_3 and CuO nano-fluids with different concentration ratios, respectively. It is observed that the Al_2O_3 nano-fluid with small volume fraction has a highest nucleation site density and this density decreases with increasing of the volume fraction. For CuO nano-fluid the nucleate site density increases as the heat flux increases for different values of the volume fraction ratio as shown in Fig. 14. The volume fraction of 0.06 % has a higher nucleate site than density that of 0.02 % and 0.2 % and still the demineralized water has a higher value in comparison with nano-fluids for all values of concentration. Fig. 15 shows that for the demineralized water, the nucleation site density was found to be higher than the Al_2O_3 and CuO nano-fluid for 0.2 % volume fraction

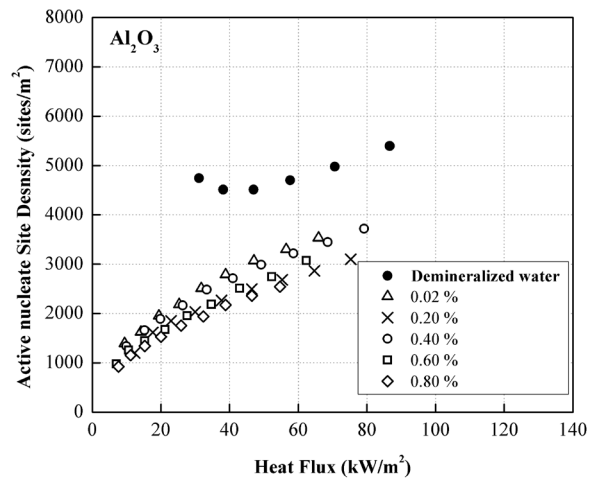


Fig. 13 Active nucleation site density calculated from the Stephan correlation for demineralized and Al_2O_3 nanofluid

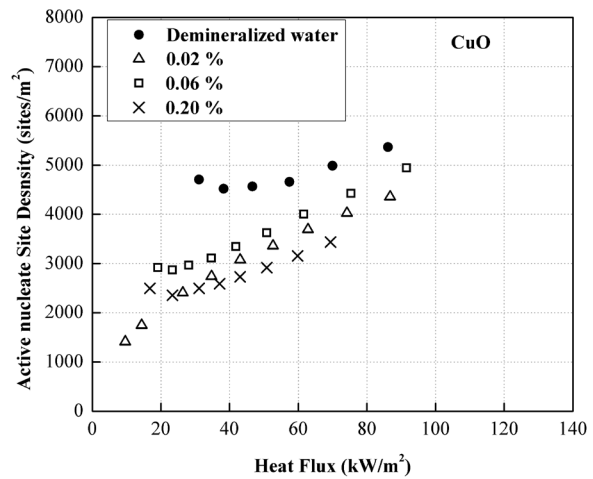


Fig. 14 Active nucleation site density calculated from the Stephan correlation for demineralized and CuO nanofluid

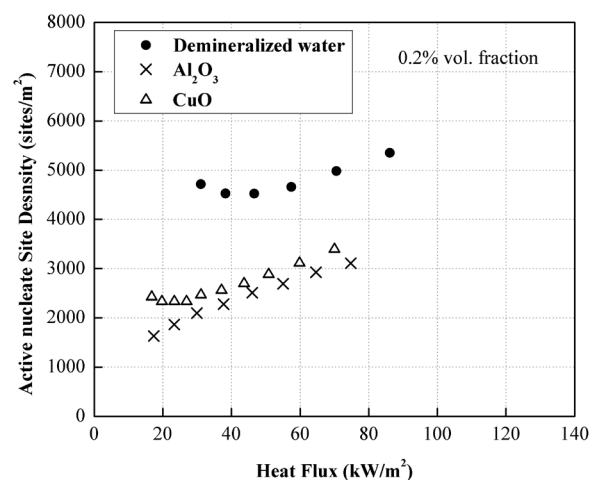


Fig. 15 Comparison of active nucleation site density calculated from the Mikic-Rohsenow correlation for Al_2O_3 and CuO nano-fluids

for different values of heat flux. The nucleation site density for CuO nano-fluid concentration was higher than that for Al_2O_3 . For a given wall superheating, the Al_2O_3 and CuO nano-fluids have a significantly lower nucleation site density with respect to demineralized water that matched well with the scanning electron microscope analysis that shows the porous nano-particle layers formation due to particle deposition during boiling. This demonstrated that the decrease in nucleation site density is potentially the cause of the degradation in boiling performance.

4 Conclusion

Experimental boiling tests for demineralized water and a water based nano-fluids with suspended Al_2O_3 and CuO nano-particles have been studied to determine the thermal boiling performance of a heated circular surface. After nano-fluid boiling test the average roughness increase observed from an initial value of 0.5 μm for the baseline to 28 μm after the final test. Nano-particles deposited on the heating surface and form a porous layer during nucleate boiling and this phenomenon decline the boiling heat transfer performance. Pool boiling heat transfer coefficient of Al_2O_3 and CuO nano-fluid measured on the aluminium alloy circular surface in the pool was compared to the coefficient of demineralized water. As presented above, Al_2O_3 and CuO nano-particles addition of water caused a decrease of the pool nucleate boiling heat transfer through the volume fraction ratio ranges 0.02 % to 0.8 % and 0.02 % to 0.20 %, respectively. The creation of a nano-particle layer on the heated surface is shown to dramatically affect the boiling performance of water. The heat transfer coefficient was decreased by increasing particle concentration.

Nomenclature

A	cross-section area of boiling surface, (m^2)
C_p	specific heat, ($\text{kJ/kg}\cdot^\circ\text{C}$)
D	aluminum alloy heating element diameter, (m)
D_d	bubble departure diameter, (m)

References

- [1] Ahmad, S. W., Karayiannis, T. G., Kenning, D. B. R., Luke, A. "Compound effect of EHD and surface roughness in pool boiling and CHF with R-123", Applied Thermal Engineering, 31(11-12), pp. 1994–2003, 2011.
<https://doi.org/10.1016/j.applthermaleng.2011.03.005>
- [2] Cieslinski, J. T., Kaczmarczyk, T. Z. "Pool boiling of water- Al_2O_3 and water-Cu nanofluids on horizontal smooth tubes", Nanoscale Research Letters, 6, article ID: 220, 2011.
<https://doi.org/10.1186/1556-276x-6-220>
- [3] Pal, S., Bhaumik, S. "Development of Theoretical Correlation for Prediction of Boiling Heat Transfer Using TiO_2 -Water Nanofluid", In: 2012 International Conference on Environment, Energy and Biotechnology, Vol. 33, Kuala Lumpur, Malaysia, 2012, pp. 34–38. [online] Available at: <http://www.ipcbee.com/vol33/007-ICEEB2012-B017.pdf> [Accessed: 05 February 2019]
- [4] Ribatski, G., Thome, J. R. "Nucleate boiling heat transfer of R134a on enhanced tubes", Applied Thermal Engineering, 26(10), pp. 1018–1031, 2006.
<https://doi.org/10.1016/j.applthermaleng.2005.09.021>

C_{sf}	experimental constant
f	frequency, (1/Sec)
g	gravitational acceleration, (m/s^2)
h	heat transfer coefficient, ($\text{W/m}^2\cdot^\circ\text{C}$)
h_{fg}	latent heat, (kJ/kg)
k	thermal conductivity, ($\text{W/m}\cdot^\circ\text{C}$)
No	active nucleation site density, (site/ m^2)
Pr	Prandtl number
T	temperature, ($^\circ\text{C}$)

Greek letter

σ	surface tension, (N/m)
β	contact angle, (35°)
ρ	density, (kg/m^3)
μ	viscosity, (N.s/m)
ϕ	volume fraction
q	heat flux density, (W/m^2)
P	electric power, (Watt)
A	heated surface area, (m^2)
h	heat transfer coefficient, ($\text{W/m}^2\cdot^\circ\text{C}$)

Subscripts

f	base-fluid
l	liquid
m	mass
nf	nano-fluids
ρ	nano-particle
sat	saturation
v	vapour
w	wall or boiling surface
ρ_f	fluid

Abbreviations

CHF	Critical Heat Flux
-----	--------------------

Acknowledgement

This work was supported by the Faculty of Engineering – Benha University and the authors would like to thank Professor Abdallah Hanafi for his continuous valuable comments.

- [5] Kavitha, T., Rajendran, A., Durairajan, A., Shanmugam, A. "Heat Transfer Enhancement Using Nano Fluids and Innovative Methods - An Overview", *International Journal of Mechanical Engineering and Technology*, 3(2), pp. 769–782, 2012. [online] Available at: https://www.iaeme.com/MasterAdmin/UploadFolder/IJMET_03_02_076/IJMET_03_02_076.pdf [Accessed: 05 February 2019]
- [6] Ciesliński, J. T., Kaczmarczyk, T. Z. "Pool boiling of nanofluids on rough and porous coated tubes: experimental and correlation", *Archives of Thermodynamics*, 35(2), pp. 3–20, 2014. <https://doi.org/10.2478/aoter-2014-0010>
- [7] Ciloglu, D., Bolukbasi, A. "A comprehensive review on pool boiling of nanofluids", *Applied Thermal Engineering*, 84, pp. 45–63, 2015. <https://doi.org/10.1016/j.applthermaleng.2015.03.063>
- [8] Salari, E., Peyghambarzadeh, M., Sarafraz, M. M., Hormozi, F. "Boiling Heat Transfer of Alumina Nano-Fluids: Role of Nanoparticle Deposition on the Boiling Heat Transfer Coefficient", *Periodica Polytechnica Chemical Engineering*, 60(4), pp. 252–258, 2016. <https://doi.org/10.3311/PPch.9324>
- [9] Ali, H. M., Generous, M. M., Ahmad, F., Irfan, M. "Experimental investigation of nucleate pool boiling heat transfer enhancement of TiO₂-water based nanofluids", *Applied Thermal Engineering*, 113, pp. 1146–1151, 2017. <https://doi.org/10.1016/j.applthermaleng.2016.11.127>
- [10] Kshirsagar, J. M., Shrivastava, R. "Experimental investigation of nucleate pool boiling characteristics of high concentrated alumina/water nanofluids", *Heat and Mass Transfer*, 54(6), pp. 1779–1790, 2018. <https://doi.org/10.1007/s00231-017-2253-7>
- [11] Moreira, T. A., Moreira, D. C., Ribatski, G. "Nanofluids for heat transfer applications: a review", *Journal of the Brazilian Society of Mechanical Sciences and Engineering*, 40, article ID: 303, 2018. <https://doi.org/10.1007/s40430-018-1225-2>
- [12] Nazari, A., Saedodin, S. "An experimental study of the nano-fluid pool boiling on the aluminium surface", *Journal of Thermal Analysis and Calorimetry*, 135(3), pp. 1753–1762, 2019. <https://doi.org/10.1007/s10973-018-7609-9>
- [13] Saad, M. K., Lezsovits, F. "Boiling Heat Transfer of Nanofluids - A Review of Recent Studies", *Thermal Science*, 23(1), pp. 109–124, 2019. <https://doi.org/10.2298/TSCI170419216K>
- [14] Xuan, Y., Roetzel, W. "Conceptions for heat transfer correlation of nanofluids", *International Journal of Heat and Mass Transfer*, 43(19), pp. 3701–3707, 2000. [https://doi.org/10.1016/S0017-9310\(99\)00369-5](https://doi.org/10.1016/S0017-9310(99)00369-5)
- [15] Maxwell, J. C. "A Treatise on Electricity and Magnetism", Vol. 1, Clarendon Press, Oxford, UK, 1873.
- [16] Holman, J. P. "Experimental Methods for Engineers", 4th ed., McGraw-Hill Book Company, New York, USA, 1984.
- [17] Gerardi, C., Buongiorno, J., Hu, L.-w., McKrell, T. "Infrared thermometry study of nanofluid pool boiling phenomena", *Nanoscale Research Letters*, 6, article ID: 232, 2011. <https://doi.org/10.1186/1556-276x-6-232>
- [18] Cieslinski, J. T., Kaczmarczyk, T. Z. "The Effect of Pressure on Heat Transfer during Pool Boiling of Water-Al₂O₃ and Water-Cu Nanofluids on Stainless Steel Smooth Tube", *Chemical and Process Engineering*, 32(4), pp. 321–332, 2011. <https://doi.org/10.2478/v10176-011-0026-2>
- [19] Das, S. K., Putra, N., Roetzel, W. "Pool boiling characteristics of nano-fluids", *International Journal of Heat and Mass Transfer*, 46(5), pp. 851–862, 2003. [https://doi.org/10.1016/s0017-9310\(02\)00348-4](https://doi.org/10.1016/s0017-9310(02)00348-4)
- [20] Bang, I. C., Heung Chang, S. "Boiling heat transfer performance and phenomena of Al₂O₃-water nano-fluids from a plain surface in a pool", *International Journal of Heat and Mass Transfer*, 48(12), pp. 2407–2419, 2005. <https://doi.org/10.1016/j.ijheatmasstransfer.2004.12.047>
- [21] Mikic, B. B., Rohsenow, W. M. "A New Correlation of Pool-Boiling Data Including the Effect of Heating Surface Characteristics", *Journal of Heat Transfer*, 91(2), pp. 245–250, 1969. <https://doi.org/10.1115/1.3580136>